Article

Cancer Cell

Regulation of Glutamine Carrier Proteins by RNF5 Determines Breast Cancer Response to ER Stress-Inducing Chemotherapies

Graphical Abstract

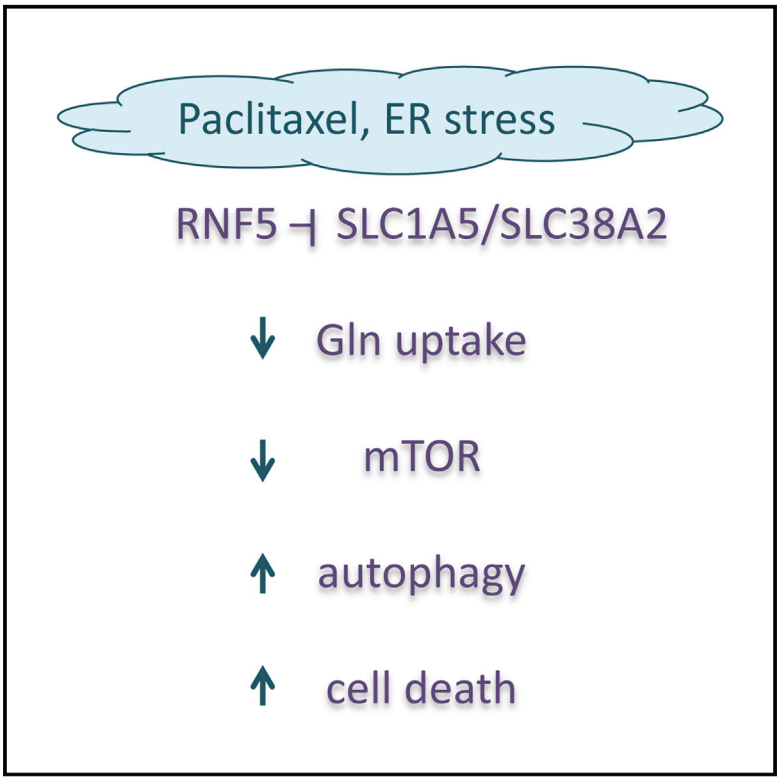

Authors

Young Joo Jeon, Sihem Khelifa, ..., Yuval Kluger, Ze'ev A. Ronai

Correspondence

ronai@sbmri.org

In Brief

Jeon et al. show that paclitaxel-induced ER stress in BCa cells promotes the ubiquitin ligase RNF5 to associate with, ubiquitinate, and degrade the Gln carriers SLC1A5 and SLC38A2, thereby leading to decreased Gln uptake and increased autophagy and cell death.

Highlights

- Gln carrier proteins SLC1A5 and SLC38A2 are regulated by ubiquitin ligase RNF5
- Glutamine uptake and mTOR activity following ERS is RNF5-SLC1A5 dependent
- RNF5 inhibition of SLC1A5 is required for paclitaxel-induced apoptosis of BCa cells
- Low SLC1A5 expression in BCa TMA and RPPA associates with good prognosis

Jeon et al., 2015, Cancer Cell *27*, 354–369
March 9, 2015
http://dx.doi.org/10.1016/j.ccell.2015.02.006

CellPress

CellPress

Cancer Cell
Article

Regulation of Glutamine Carrier Proteins by RNF5 Determines Breast Cancer Response to ER Stress-Inducing Chemotherapies

Young Joo Jeon,[1] Sihem Khelifa,[2] Boris Ratnikov,[1] David A. Scott,[1] Yongmei Feng,[1] Fabio Parisi,[2] Chelsea Ruller,[1] Eric Lau,[1] Hyungsoo Kim,[1] Laurence M. Brill,[1] Tingting Jiang,[2] David L. Rimm,[2] Robert D. Cardiff,[3] Gordon B. Mills,[4] Jeffrey W. Smith,[1] Andrei L. Osterman,[1] Yuval Kluger,[2] and Ze'ev A. Ronai[1,*]

[1]Tumor Initiation and Maintenance Program, Cancer Center, Sanford-Burnham Medical Research Institute, La Jolla, CA 92037, USA
[2]Department of Pathology, Yale University, New Haven, CT 06510, USA
[3]Department of Pathology, University of California, Davis, Davis, CA 95616, USA
[4]Department of Systems Biology, MD Anderson Cancer Center, Houston, TX 77030, USA
*Correspondence: ronai@sbmri.org
http://dx.doi.org/10.1016/j.ccell.2015.02.006

SUMMARY

Many tumor cells are fueled by altered metabolism and increased glutamine (Gln) dependence. We identify regulation of the L-glutamine carrier proteins SLC1A5 and SLC38A2 (SLC1A5/38A2) by the ubiquitin ligase RNF5. Paclitaxel-induced ER stress to breast cancer (BCa) cells promotes RNF5 association, ubiquitination, and degradation of SLC1A5/38A2. This decreases Gln uptake, levels of TCA cycle components, mTOR signaling, and proliferation while increasing autophagy and cell death. *Rnf5*-deficient *MMTV-PyMT* mammary tumors were less differentiated and showed elevated SLC1A5 expression. Whereas RNF5 depletion in MDA-MB-231 cells promoted tumorigenesis and abolished paclitaxel responsiveness, SLC1A5/38A2 knockdown elicited opposing effects. Inverse RNF5^{hi}/SLC1A5/38A2^{lo} expression was associated with positive prognosis in BCa. Thus, RNF5 control of Gln uptake underlies BCa response to chemotherapies.

INTRODUCTION

The ER stress (ERS) response plays a critical role in normal cellular homeostasis by governing cell commitment to survival or death in response to internal or external cues (Ron and Walter, 2007; Tabas and Ron, 2011). ERS homeostasis is maintained through the unfolded protein response (UPR), an adaptive intracellular signaling pathway that responds to stress stimuli (Wang et al., 2010). Notably, ERS pathway components are deregulated in almost every pathological disorder, including metabolic, neurodegenerative, and inflammatory diseases and cancer (Hotamisligil, 2010). Resolution of the ERS response and UPR, which are induced by specific chemotherapeutic drugs, is achieved by commitment to survival, autophagy, or death programs (Meusser et al., 2005; Ogata et al., 2006).

Several dedicated ubiquitin ligases play critical roles in the ERS response and UPR. One of those is RNF5, an ER-associated E3 ubiquitin ligase that regulates stability and clearance of proteins functioning in various cellular processes. RNF5 is part of the UBC6e/p97 network, which are key components of ER-associated degradation (ERAD) (Bernasconi et al., 2013). RNF5 contributes to clearance of misfolded proteins (Grove et al., 2011; Younger et al., 2006). Increased RNF5 expression is linked to advanced breast cancer (BCa) (Bromberg et al., 2007).

Intracellular Gln levels are controlled by membrane-anchored glutamine (Gln) transporters that mediate uptake of small aliphatic amino acids such as L-Gln (Taylor et al., 2003). L-Gln is a critical nutrient for cancer cells (Medina, 2001), serving as a carbon and nitrogen source for synthesis of macromolecules

Significance

Understanding the mechanisms underlying tumor cell responsiveness to therapy is expected to allow stratification of patients for personalized treatment. Here, we identify two glutamine carrier proteins, SLC1A5 and SLC38A2 (SLC1A5/38A2), that undergo ubiquitination-dependent degradation mediated by the ubiquitin ligase RNF5 in response to ER stress induced by specific chemotherapies (illustrated here by paclitaxel). Once the carrier proteins are degraded, glutamine uptake is reduced, resulting in mTOR inhibition and activation of autophagy and cell death programs. We demonstrate the importance of RNF5 in antagonizing tumor development, progression, and response to therapy using human BCa tissues and genetic mouse models. RNF5^{hi}/SLC1A5^{lo} expression is associated with luminal type BCa and improved prognosis, pointing to possible stratification of BCa patients for therapies.

and, via conversion to α-ketoglutarate, as an ATP source through the tricarboxylic acid cycle (TCA) cycle and oxidative phosphorylation. L-Gln metabolism is transcriptionally regulated by Myc (Gao et al., 2009; Wise et al., 2008), which also suppresses microRNA-23a/b to enhance expression of the glutaminase 1 (GLS1) (Liu et al., 2012).

Among Gln transporters, SLC1A5 is highly expressed in BCa cells and is also implicated in regulation of essential amino acid influx, mammalian target of rapamycin (mTOR) activation (Nicklin et al., 2009), and L-Gln-dependent tumor cell growth (Hassanein et al., 2013). Moreover, SLC1A5 inhibition in hepatoma and acute myeloid leukemia cells attenuates mTORC1 signaling, resulting in growth repression and apoptosis (Fuchs et al., 2007; Willems et al., 2013), suggesting a role in cellular transformation (Witte et al., 2002). Mechanisms underlying control of SLC1A5-mediated L-Gln uptake in tumor cells and implications for the tumor cell response to therapy are largely unknown (DeBerardinis et al., 2007). The glutamine transporter SLC38A2 is more ubiquitously expressed, although elevated SLC38A2 expression has been reported in prostate tumors (Okudaira et al., 2011). Intracellular L-Gln levels maintained by both SLC1A5 and SLC38A2 (SLC1A5/38A2) in turn modulate activity of the amino acid exchanger SLC7A5/SLC3A2 and promote leucine uptake (Baird et al., 2009), with a concomitant effect on mTOR signaling (Evans et al., 2008).

Here, we set out to determine the role of RNF5 in the control of two L-Gln transporters, SLC1A5/38A2, and its implications for L-Gln uptake and BCa response to therapy.

RESULTS

SLC1A5/38A2 Are RNF5 Substrates

To identify RNF5 substrate(s) in BCa cells, we overexpressed a FLAG-tagged catalytically inactive RING mutant form of RNF5 (RNF5 RM) in the human BCa cell line MCF7. Coimmunoprecipitating proteins (Figure S1A) were subjected to liquid chromatography-tandem mass spectrometry (LC-MS/MS) analysis, which identified peptides corresponding to SLC1A5/38A2 proteins (data not shown). To confirm interaction of SLC1A5/38A2 with RNF5, we performed immunoprecipitations (IPs) using exogenous and endogenous proteins. SLC1A5/38A2 bound to both wild-type (WT) RNF5 and RNF5 RM, but not to RNF5 ΔCT, which lacks the C-terminal transmembrane domain (Figures 1A and 1B). These findings confirm association of RNF5 with SLC1A5/38A2 and demonstrate that the RNF5 membrane anchor is required for the interaction, consistent with RNF5 interactions with other substrates (Kuang et al., 2012). To determine whether RNF5 ubiquitinates SLC1A5/38A2, we co-expressed SLC1A5 or SLC38A2 with hemagglutinin (HA)-tagged ubiquitin plus WT, RM, or ΔCT forms of RNF5. Both SLC1A5 and SLC38A2 were ubiquitinated by WT RNF5, but not by RNF5 RM or RNF5 ΔCT (Figures 1C and 1D), indicating that ligase activity and membrane anchor are required for RNF5 effects on these Gln carrier proteins. Accordingly, steady-state levels of SLC1A5 or SLC38A2 proteins decreased as RNF5 levels increased (Figures 1E and 1F). Degradation of SLC1A5 or SLC38A2 by RNF5 was blocked in cells treated with the proteasome inhibitor MG132 (Figures 1E and 1F), consistent with RNF5-induced ubiquitination of SLC1A5 and SLC38A2, resulting in proteasome-mediated degradation. LC-MS/MS analysis also identified the bi-directional transporter SLC3A2 as a putative RNF5-interacting protein. Although IP analysis confirmed RNF5 interaction with SLC3A2 (Figure S1B), RNF5 did not promote SLC3A2 ubiquitination (Figure S1C). To determine whether RNF5 activity alters SLC1A5 half-life, HEK293T cells were co-transfected with SLC1A5 plus WT, RM, or ΔCT RNF5 and then treated with the translational inhibitor cycloheximide for varying times. As expected, ectopically expressed WT RNF5, but not RM or ΔCT, decreased SLC1A5 half-life from 8 to 2 hr (Figures 1G and 1H). These findings demonstrate that RNF5 association leads to ubiquitination and degradation of SLC1A5/38A2.

ERS Promotes RNF5/SLC1A5 Association and RNF5-Dependent Ubiquitination and Degradation of SLC1A5 in BCa Cells

We next searched for conditions favoring RNF5 regulation of SLC1A5 in BCa cells. Treatment of MDA-MB-231 (human triple-negative) BCa cells with three well-established ERS inducers—brefeldin A (BFA), tunicamycin (TM), or thapsigargin (TG)—promoted a marked and time-dependent decrease in SLC1A5 levels (Figure 2A). Since TG was less potent in regulating Gln carrier proteins than BFA or TM, we assessed the effect of increasing TG doses and demonstrate a corresponding dose-dependent decrease in the levels of SLC1A5/38A2 (Figure S2). Co-incubation of cells with MG132 attenuated BFA effects, suggesting that SLC1A5 undergoes proteasome-dependent degradation in response to ERS (Figure 2B). Consistent with this finding, BFA treatment decreased SLC1A5 half-life from >8 to ~2.5 hr (Figure 2C).

Given that ERS-inducing agents reduce SLC1A5 stability, we assessed a potential role for RNF5 in this process. Notably, interaction of SLC1A5 with RNF5 increased in BFA-teated cells (Figure 2D) and in paclitaxel-treated cells (Figure 2E). BFA-induced SLC1A5 ubiquitination decreased following RNF5 knockdown (KD) relative to control small hairpin RNA (shRNA)-treated cells (Figure 2F). Likewise, BFA-, TM-, or TG-induced SLC1A5 destabilization decreased following RNF5 depletion (Figure 2G). Notably, among the three ERS inducers, BFA treatment promoted the most pronounced decrease in SLC1A5 levels. Since BFA promotes retrograde transport of proteins from the Golgi to the ER, it may increase SLC1A5 accumulation in the ER, thereby enhancing its interaction with RNF5. Collectively, these findings establish regulation of SLC1A5 stability by RNF5 in response to ERS.

ERS-Induced, RNF5-Mediated SLC1A5/38A2 Degradation Decreases Glutamine Uptake, mTOR Signaling, and BCa Cell Growth

Using gas chromatography (GC)-MS analysis, we observed that restoration of the Gln pool (to cells that were deprived of glutamine followed by replenishment by glutamine-rich media) occurred rapidly (Figure S3A). The steady-state Gln levels (reached within 1 hr) did not differ appreciably between cells with perturbed versus unperturbed uptake machinery. Owing to the slower conversion of glutamine to glutamate, we chose to assess glutamate and downstream metabolites in cells that were subjected to KD of RNF5, SLC1A5, or SLC38A2 individually

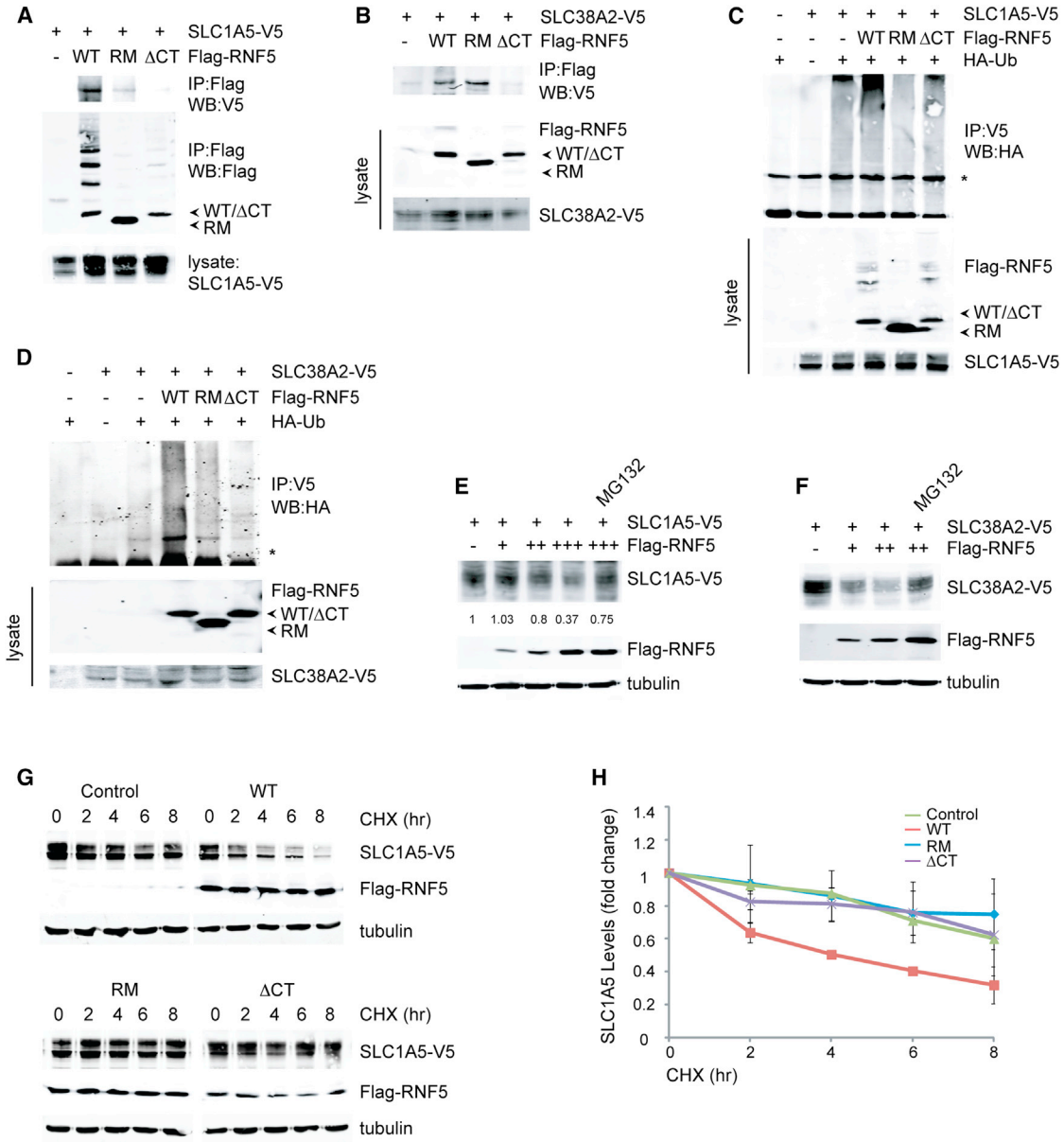

Figure 1. RNF5 Ubiquitinates and Destabilizes the Gln Carrier Proteins SLC1A5 and SLC38A2

(A and B) V5-tagged SLC1A5 (SLC1A5-V5) (A) or V5-tagged SLC38A2 (SLC38A2-V5) (B) was transiently co-expressed with FLAG-tagged RNF5 WT, RNF5 RM, or RNF5 ΔCT in HEK293T cells. Cells were treated (10 μM MG132, 4 hr) and cell lysates were subjected to IP followed by WB with indicated antibodies.

(C and D) SLC1A5-V5 (C) or SLC38A2-V5 (D) was co-expressed in HEK293T cells with HA-ubiquitin (Ub) plus indicated RNF5 constructs. Cells were treated with MG132 (10 μM, 4 hr) prior to preparation of lysates and then subjected to IP followed by WB using indicated antibodies. Asterisk indicates immunoglobulin G heavy chain.

(E and F) HEK293T cells expressing SLC1A5-V5 (E) or SLC38A2-V5 (F) were transfected with increasing amounts of FLAG-RNF5 WT and treated as indicated with MG132 (10 μM, 4 hr). WB performed with indicated antibodies.

(G and H) HEK293T cells were transfected with SLC1A5-V5 and either a 3×FLAG-tagged control construct or indicated RNF5 constructs and treated with cycloheximide (CHX; 50 μg/ml) for indicated times. WB performed with indicated antibodies (G), and SLC1A5 protein levels were quantified by densitometry (H). Bars represent mean values ± SD of three experiments.

See also Figure S1.

or in combination. Notably, combined SLC1A5/38A2 KD decreased the initial rate of Gln accumulation (Figure 3A). Furthermore, combined KD of SLC1A5/38A2 plus RNF5 KD partially rescued Gln uptake (Figures 3A and S3B).

To complement our assessment of effects of RNF5 on Gln uptake and conversion to Glu, we used [^{13}C]Gln to allow flux analysis (without the need for glutamine starvation) of downstream Gln intermediates. Replacement of the unlabeled intracellular

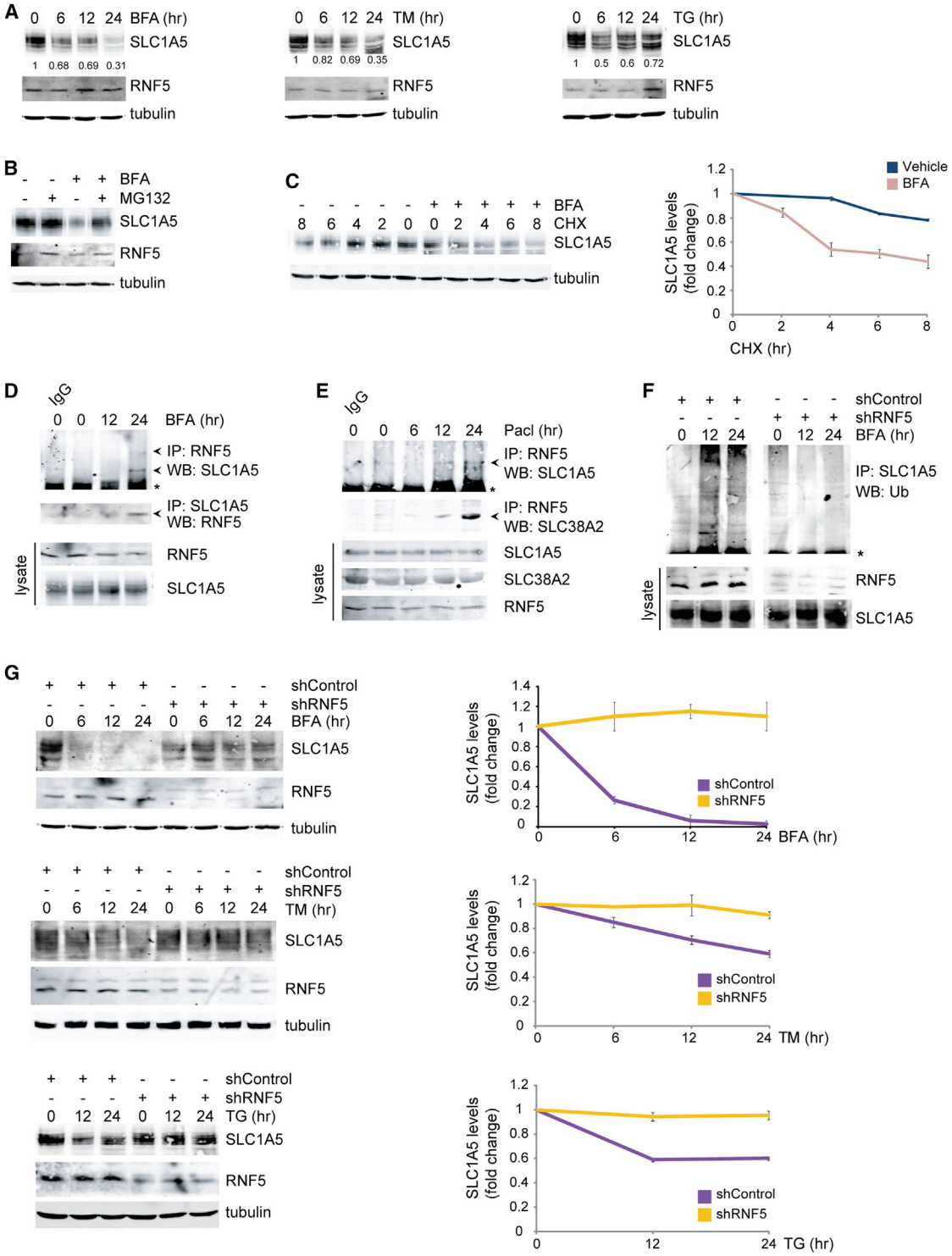

Figure 2. RNF5 Ubiquitinates and Mediates Degradation of SLC1A5 in Response to ERS

(A) MDA-MB-231 cells were treated with 2.5 μg/ml BFA, 5 μg/ml TM, or 2 μM TG for indicated times. WB performed with indicated antibodies.

(B) MDA-MB-231 cells were treated with BFA (2.5 μM, 24 hr) in the absence or presence of MG132 (10 μM, 4 hr). WB performed with indicated antibodies.

(C) MDA-MB-231 cells were incubated with BFA (2.5 μg/ml, 12 hr) and then treated with CHX (50 μg/ml) for indicated times. Left: WB performed with indicated antibodies. Right: SLC1A5 protein levels were quantified by densitometry. Bars represent mean values ± SD of three experiments.

(D–F) Cell lysates were prepared from MDA-MB-231 cells treated with 2.5 μg/ml BFA (D) or 100 nM paclitaxel (E) or transfected with indicated shRNA and incubated with 2.5 μg/ml BFA (F) for indicated times and treated with MG132 for 4 hr before preparation of cell lysates. IP and WB were then performed with indicated antibodies. Asterisk indicates immunoglobulin G (IgG) heavy chain.

(legend continued on next page)

Gln pool with steady-state levels of [^{13}C]Gln (Figure S3C) revealed only a minor difference between paclitaxel-treated and untreated MDA-MB-231 cells (Figure 3B, left graph). Nonetheless, monitoring glutamate and downstream TCA intermediates under these experimental conditions allowed us to identify a significant (>30% at the 1-hr time point) decrease in ^{13}C enrichment of downstream products upon paclitaxel treatment (Figure 3B, right graph). To substantiate these observations, we used radiolabeled glutamine ([^{3}H]Gln) in MDA-MB-231 cells where expression of RNF5 and Gln carrier proteins was altered. To better capture the changes in intracellular Gln levels, cells were also treated with 2-aminobicyclo-(2,2,1)-heptane-2-carboxylic acid (BCH), an inhibitor of glutamine exporter SLC7A5 (Nicklin et al., 2009). Notably, paclitaxel treatment reduced levels of intracellular [^{3}H]Gln (Figure 3C). Levels of intracellular [^{3}H]Gln increased in cells expressing shRNF5 (Figures 3C and S3D), which was attenuated following paclitaxel treatment; however, the resultant [^{3}H]Gln levels were still higher than basal [^{3}H]Gln levels. Notably, in the absence of BCH, changes seen upon paclitaxel before and after shRNF5 were minimal (Figure S3E), pointing to the rapid export of intracellular Gln. Significantly, KD of SLC1A5 and SLC38A2 reduced the level of intracellular [^{3}H]Gln before and after paclitaxel treatment (Figure 3C), which was further reduced upon repeated transfection of small interfering SLC38A2 (Figure S3E). KD of RNF5 in SLC1A5/38A2 KD cells did not affect intracellular levels in the presence of BCH, yet cause some increase in glutamine levels without BCH (Figure S3E). These results demonstrate that RNF5 controls the levels of intracellular Gln through its effect on SLC1A5/38A2 and that reduced glutamine uptake following paclitaxel treatment is primarily RNF5 and SLC1A5/38A2 dependent.

As availability of intracellular amino acids controls mTOR activity (Kim et al., 2013), we analyzed mTOR signaling upon KD of RNF5 or SLC1A5 in BFA-treated MDA-MB-231 cells. Phosphorylation of mTOR and its targets S6K and 4EBP1 decreased in control shRNA-expressing cells following BFA treatment, concomitant with decreased SLC1A5 expression (Figure 3D). Notably, SLC1A5 KD in the absence of BFA treatment also blocked activation of mTOR and its downstream targets. In contrast, RNF5 KD led to persistent activation of mTOR signaling, coinciding with SLC1A5 stabilization, an effect attenuated by simultaneous SLC1A5 KD (Figure 3D).

Given the effect of the RNF5-SLC1A5/38A2 regulatory axis on Gln metabolism and mTOR activity, we assessed changes in growth and colony formation of BCa cells with altered levels of RNF5 and SLC1A5/38A2. Whereas BFA treatment inhibits cell proliferation, this effect was attenuated by RNF5 KD, but not by SLC1A5 KD. Notably, simultaneous KD of RNF5 and SLC1A5 rescued the effects of RNF5 KD alone (Figure 3E). We obtained similar results when we examined clonogenic growth of MDA-MB-231 or MCF7 cells after BFA treatment (Figures 3F and S3F). Once again, the effect of RNF5 KD was attenuated upon SLC1A5 KD (Figure 3F). Rapamycin treatment suppressed phosphorylation of S6K and 4EBP1 in BFA-treated cells expressing shRNF5 (Figure 3G), and treatment with BFA plus rapamycin inhibited clonogenic growth of shRNF5-expressing cells, whereas BFA treatment alone did not (Figure 3H). These results suggest that RNF5 regulation of SLC1A5 occurs upstream of mTOR signaling.

RNF5-Dependent Downregulation of SLC1A5 or SLC38A2 in BCa Cells Is Associated with Paclitaxel-Dependent Protein Misfolding

Next, we examined SLC1A5, SLC3A2, SLC38A2, and RNF5 expression in a set of BCa cell lines (Figure 4A). MCF7, MDA-MB-231, and SKBR-3 lines showed high RNF5 expression, whereas expression was lower in MDA-MB-453, MDA-MB-468, and T47D lines. Notably, we did not observe an inverse relationship between SLC1A5 or SLC38A2 expression versus RNF5 expression under normal growth conditions. Since we observed an effect of RNF5 on SLC1A5 and SLC38A2 after exposure to ERS-inducing treatments, we asked whether treatment with cisplatin, doxorubicin, or paclitaxel, which are commonly used BCa chemotherapies, would modulate the RNF5-SLC1A5/38A2 axis. Using BCa cell lines representing high (MCF7 and MDA-MB-231) and low (MDA-MB-453 and T47D) RNF5 levels, we found that SLC1A5 expression markedly decreased in high RNF5-expressing lines relative to low-expressing lines after paclitaxel treatment and to a lesser extent following cisplatin or doxorubicin treatment. SLC38A2 expression was also affected to greater degree in high RNF5-expressing lines following paclitaxel and doxorubicin treatment and to a lesser degree by cisplatin (Figure 4B). Consistent with our earlier analysis, we observed no apparent relationship between RNF5 expression and a third Gln carrier protein, SLC3A2 (Figure S1C), even following drug treatment (Figure 4B). Differential effects of chemotherapeutic drugs on SLC1A5 and SLC38A2 expression in BCa cells suggest that RNF5 and SLC1A5/38A2 expression may serve as useful markers for patient stratification and possibly prognostication.

We next assessed possible mechanisms that may account for the reduced level of SLC1A5 following doxorubicin and paclitaxel. First, we excluded the possibility that RNF5 exhibits different subcellular localization in lines where SLC1A5 levels were reduced following paclitaxel (Figure S4A). Given that ERS promotes RNF5-mediated SLC1A5 degradation, we asked whether paclitaxel induces ERS and found that ERS was induced by paclitaxel in MDA-MB-231 cells, but not in MDA-MB-453 cells (Figure 4C), consistent with effects of paclitaxel on SLC1A5 degradation. Canonical branches of the UPR are mediated by inositol-requiring enzyme 1 (IRE1α, IRE1β), protein kinase RNA-like ER kinase (PERK), and activating transcription factor 6 (ATF6) (Hetz et al., 2013; Walter and Ron, 2011). Activated PERK phosphorylates eukaryotic translation initiation factor 2α (eIF2α), silencing translation. Treatment of MDA-MB-231 cells with paclitaxel markedly increased IRE1α and eIF2α phosphorylation, without altering levels of chaperones such as binding immunoglobulin heavy chain-binding protein (BiP), protein

(G) MDA-MB-231 cells were transfected with shControl or shRNF5 and incubated with 2.5 μg/ml BFA, 5 μg/ml TM, or 2 μM TG for indicated times. Left: WB performed with indicated antibodies. Right: SLC1A5 protein levels were quantified by densitometry. Bars represent mean values ± SD of three independent experiments.
See also Figure S2.

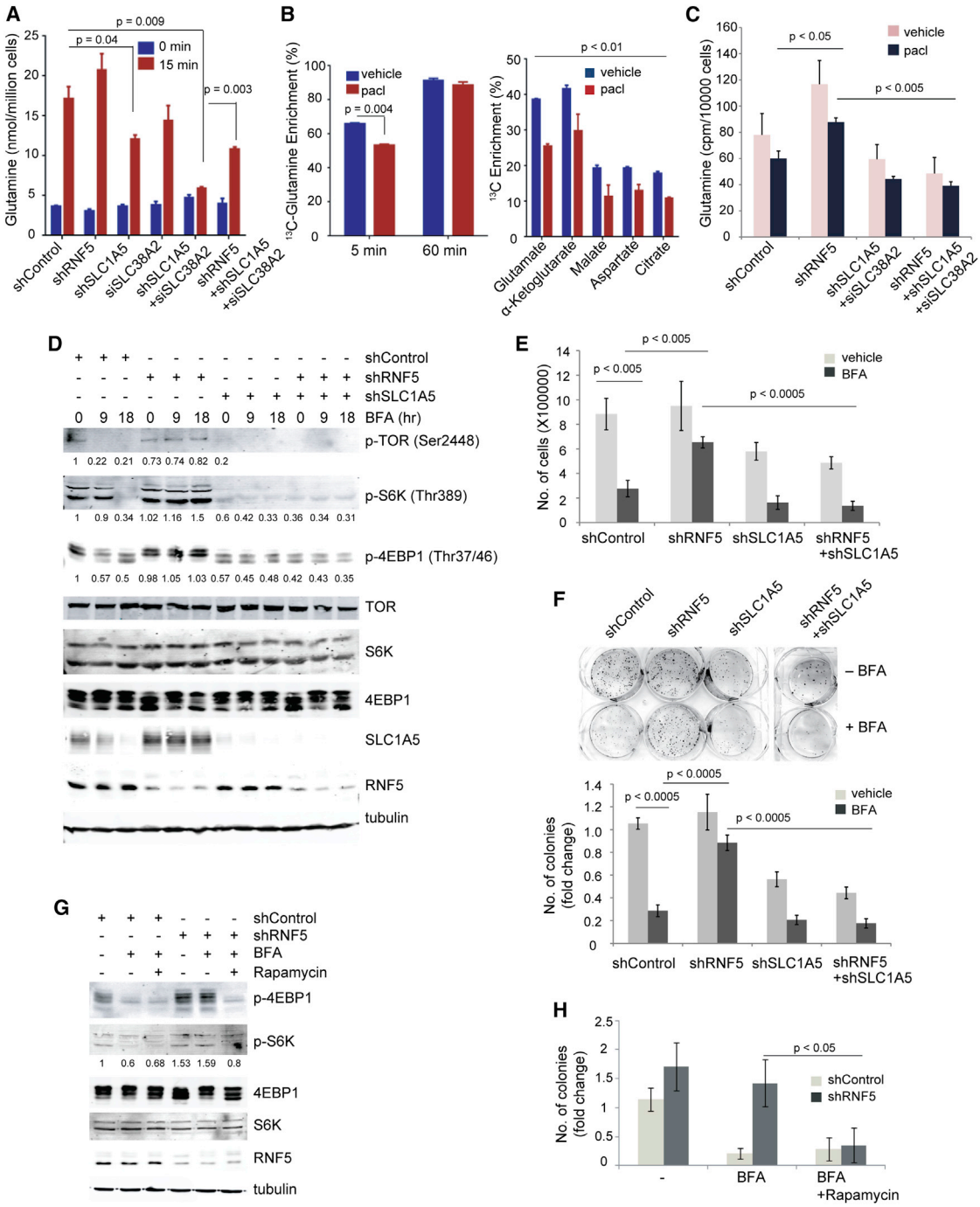

Figure 3. RNF5-Mediated SLC1A5 Degradation Downregulates L-Glutamine Uptake, mTOR Signaling, and Cell Proliferation in Response to ERS

(A) MDA-MB-231 cells transfected with indicated constructs were incubated for 6 hr with media lacking Gln, followed by media supplemented with 1 mM Gln for 15 min before cells were harvested. Levels of intracellular L-Gln were quantified using GC-MS. Bars represent the mean ± SD.

(B) MDA-MB-231 cells were incubated with 100 nM paclitaxel for 24 hr and then subjected to incubation in medium containing 1 mM [^{13}C]glutamine (50% labeled). Intracellular [^{13}C]glutamine and [^{13}C]glutamine-derived metabolites were measured by GC-MS. Bars represent the mean ± SD.

(C) MDA-MB-231 cells transfected with indicated constructs were treated with paclitaxel (100 nM, 18 hr) and BCH (10 mM for 1 hr prior to addition on radiolabeled Gln) and then incubated in medium containing [^{3}H]Gln (5 μCi/ml, 15 min). Duplicate samples were subjected to liquid scintillation assay. Bars represent the mean ± SD.

(D) MDA-MB-231 cells transfected with indicated constructs were incubated for indicated times with or without 2.5 μg/ml BFA. WB performed with indicated antibodies.

(E) MDA-MB-231 cells transfected with the indicated constructs were incubated with or without BFA for 24 hr. Viable cells were counted using trypan blue exclusion. Bars represent the mean ± SD of three independent experiments.

(legend continued on next page)

disulfide isomerase (PDI), or Ero1-Lα (Figure 4C). Surprisingly, unlike paclitaxel, doxorubicin treatment did not induce ERS or alter downstream UPR effectors in MDA-MB-231 cells, suggesting that paclitaxel-induced ERS, but not doxorubicin-induced ERS, underlies RNF5-dependent SLC1A5 degradation. Consistent with a requirement for ERS in SLC1A5 degradation, neither doxorubicin nor paclitaxel treatment induced ERS in MDA-MB-453 cells, suggesting that the ability to activate ERS constitutes another layer of control of SLC1A5 degradation (Figure 4C). To further assess a link between RNF5-SLC1A5/38A2 signaling and UPR, the BCa cell lines MDA-MB-231, MDA-MB-453, and SKBR-3 were treated with paclitaxel, and then levels of Gln carrier proteins were monitored over time. SLC1A5/38A2 levels markedly decreased following paclitaxel treatment in MDA-MB-231 cells, but not in MDA-MB-453 cells (Figure 4D). Of interest, SLC1A5/38A2 levels decreased 36 hr after paclitaxel treatment in SKBR-3 cells, although RNF5 levels in these cells are comparable to those in MDA-MB-231 cells. Assessment of UPR activation in these cells revealed that while IREα and eIF2α phosphorylation did not change after paclitaxel treatment of SKBR-3 cells, they were induced in MDA-MB-231 cells (Figure 4E). These findings suggest that UPR activation is indispensable for RNF5-mediated SLC1A5/38A2 degradation following paclitaxel treatment. Correspondingly, PERK inhibition attenuated paclitaxel-induced SLC1A5/38A2 degradation in MDA-MB-231 cells (Figure 4F).

Since RNF5 is implicated in the clearance of misfolded proteins as part of the ERAD response (Tcherpakov et al., 2009; Younger et al., 2006), we asked whether RNF5 interaction with Gln-carrier proteins required changes in protein folding following ERS. To do so, we subjected BCa cells to [^{35}S]methionine/cysteine-based labeling followed by immunopurification of [^{35}S]SLC1A5 and limited proteolytic cleavage using 2-(2′-nitrophenylsulfonyl)-3-methyl-3-bromoindolenine (BNPS)-Skatole. SDS-PAGE analysis followed by autoradiography revealed a marked decrease in SLC1A5 cleavage before but not after paclitaxel treatment (Figures 4G and S4B). These findings suggest that SLC1A5 undergoes misfolding following ERS, consistent with RNF5 recognition of misfolded proteins at the ER membrane. RNF5 KD attenuated paclitaxel-induced SLC1A5/38A2 degradation (Figure 4H). Likewise, the half-lives of both SLC1A5/38A2 increased after RNF5 KD in paclitaxel-treated MDA-MB-231 cells (Figure 4I).

Since glutamine levels also alter homeostasis of reactive oxygen species (ROS), we determined whether RNF5 control of SLC1A5/38A2 stability impacts ROS levels. ROS levels were attenuated in RNF5-depleted cells (Figures 4J and S4C). Notably, KD of either SLC1A5, SLC38A2, or their combination did not affect ROS levels, as seen upon KD of RNF5; and the combined KD of SLC1A5/38A2 and RNF5 prevented the decrease in ROS levels seen upon KD of RNF5 alone, pointing to the role of the RNF5-SLC1A5/38A2 pathway in regulating cellular ROS levels.

RNF5-Mediated SLC1A5 Degradation Promotes Autophagy and Cell Death Programs in Response to ERS

The link between ERS and autophagy, including direct activation of autophagy genes by the key component of the UPR ATF4 (B'chir et al., 2013; He and Klionsky, 2009) and mTOR as a negative regulator of autophagy (Blommaart et al., 1995), prompted us to assess whether RNF5 affects autophagy through control of SLC1A5/38A2. In support of such a possibility is a previous report that loss of SLC1A5 activates autophagy (Nicklin et al., 2009). To this end we monitored changes in levels of autophagy markers p62 and LC3 in BCa cells with altered expression of RNF5-SLC1A5/38A2. BFA-treated BCa cells exhibited mTOR inactivation and reduced levels of p62 as early as 9 hr after treatment, changes that were blocked by shRNF5 expression and rescued by simultaneous SLC1A5 KD (Figure 5A). Intriguingly, SLC1A5 KD, either alone or in combination with RNF5 KD, promoted p62 degradation in both the absence and presence of BFA (Figure 5A), suggesting that RNF5-mediated SLC1A5 degradation enhances ERS-induced autophagy. Consistent with changes in p62 expression, BFA treatment increased the number of LC3 punctae (monitored by GFP-microtubule-associated protein 1 light chain 3 [LC3]), an effect that was significantly inhibited by RNF5 KD (Figures 5B and 5C). Importantly, SLC1A5 depletion promoted marked increases in the number of GFP-LC3 punctae in non-treated cells and rescued punctae formation in shRNF5-expressing cells in the presence and absence of BFA (Figures 5B and 5C). Rapamycin treatment increased the number of GFP-LC3 punctae in BFA-treated, shRNF5-expressing cells, consistent with mTOR being downstream of RNF5 in the ERS-induced autophagy pathway.

Because high levels of ERS activate apoptosis (Shore et al., 2011), we asked whether the RNF5-SLC1A5 regulatory axis could also contribute to ERS-induced apoptosis in MDA-MB-231 cells. BFA treatment of control cells increased apoptosis at later time points (i.e., 18–48 hr), an activity attenuated in shRNF5-expressing cells, but not in shSLC1A5-expressing cells (Figures 5D and S5A). The effect of RNF5 depletion was attenuated upon simultaneous SLC1A5 KD. Fluorescence-activated cell sorting (FACS) analysis of BCa cells incubated with BFA revealed that reduced RNF5 expression limited the degree of apoptosis that could be rescued upon co-depletion of RNF5 and SLC1A5, thereby confirming the requirement for the RNF5-SLC1A5 regulatory axis in BFA-dependent induction of apoptosis (Figures 5E and S5B). Furthermore, SLC1A5/38A2 KD was sufficient to promote apoptosis in the absence of paclitaxel. Notably, attenuation of apoptosis upon RNF5 depletion was restored following co-depletion of SLC1A5/38A2 (Figures 5F and S5C). These findings substantiate the importance of

(F) MDA-MB-231 cells transfected as in (E) were incubated with or without BFA for 7 days. Colonies were stained with crystal violet and counted. Bars represent the mean ± SD of three independent experiments.

(G) MDA-MB-231 cells transfected with shControl or shRNF5 were treated with BFA in the absence or presence of rapamycin (1 μM, 12 hr). WB performed with indicated antibodies.

(H) MDA-MB-231 cells transfected and incubated with BFA in the absence or presence of rapamycin as in (G). One week later, colonies were stained with crystal violet and counted. Bars represent means ± SD of three independent experiments.

See also Figure S3.

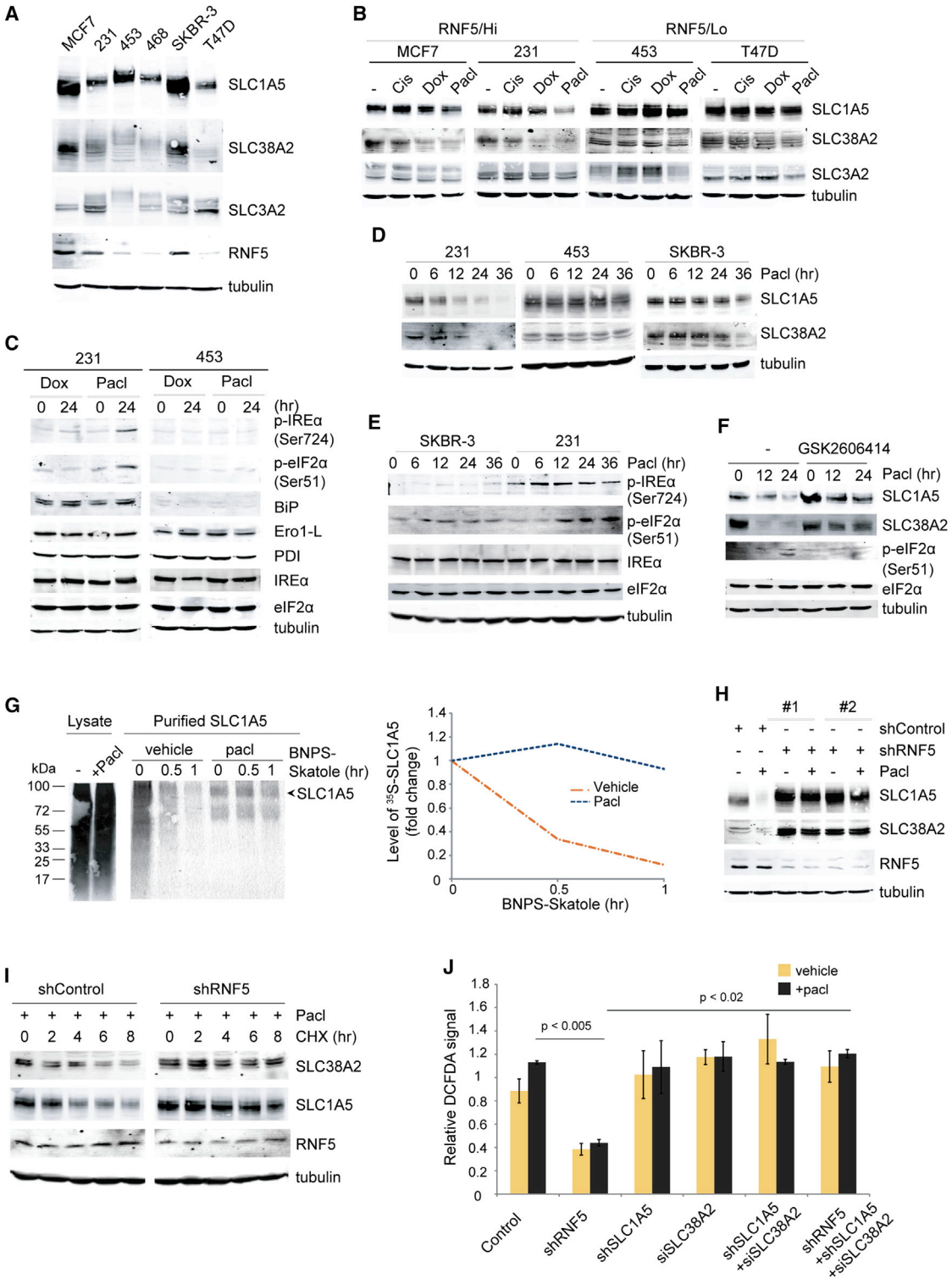

Figure 4. Paclitaxel-Induced ERS and RNF5-Dependent SLC1A5/38A2 Degradation Is Associated with Protein Misfolding

(A) Cell lysates from BCa lines MCF7, MDA-MB-231 (231), MDA-MB-453 (453), MDA-MB-468 (468), SKBR-3, or T47D were immunoblotted with indicated antibodies.

(B) Indicated cell lines were incubated with 20 μM cisplatin (Cis), 0.5 μg/ml doxorubicin (Dox), or 100 nM paclitaxel (Pacl) for 24 hr. WB performed with indicated antibodies.

(C) Indicated cell lines were incubated with doxorubicin or paclitaxel for indicated times. WB performed with indicated antibodies.

(D) Indicated cell lines were incubated with paclitaxel for indicated times. WB performed with indicated antibodies.

(legend continued on next page)

RNF5-SLC1A5/38A2 in determining BCa response to relevant chemotherapies. The ability of altered Gln metabolism to induce autophagy (at earlier time points) and cell death programs (at later time points) is consistent with studies linking these two processes (Mariño et al., 2014).

RNF5 Inhibition Promotes Mammary Tumors in the *MMTV-PyMT* Mouse Model

We next determined whether RNF5 loss affects mammary tumor development in a genetic mouse model of BCa. To do so, we crossed C57BL/6 *Rnf5*$^{-/-}$ mice with C57BL/6 mouse mammary tumor virus-polyoma middle T (MMTV-PyMT), a transgenic model of BCa that permits the examination of in situ tumor progression from hyperplasia to metastasis (Fluck and Schaffhausen, 2009). Significantly, mammary tumors from *Rnf5*$^{-/-}$ mice in this model were generally much less differentiated than those seen in *Rnf5*$^{+/+}$ mice (Figure 6A), suggesting that RNF5 loss promotes tumor development and progression. Immunostaining with vimentin, a marker of epithelial to mesenchymal transition (EMT) and of poorly differentiated tumors, confirmed that RNF5 loss is associated with less differentiated tumors and progression of the EMT program (Figure 6B). Notably, mammary tumors from *MMTV-PyMT;Rnf5*$^{-/-}$ mice exhibited more robust SLC1A5 expression and contained larger areas of SLC1A5 expression than did tumors from *MMTV-PyMT;Rnf5*$^{+/+}$ mice (Figure 6C). Consistent with the observations that RNF5-mediated SLC1A5 degradation suppresses mTOR activation (Figure 3D), mammary tumors from *MMTV-PyMT;Rnf5*$^{-/-}$ mice exhibited higher levels of phosphorylated S6, a downstream mTOR target (Figure 6D).

RNF5 Expression Is Required for BCa Response to Paclitaxel Treatment

To confirm the role of RNF5 in BCa development and response to chemotherapeutic drugs, we generated MDA-MB-231 cells that stably express shRNF5 (Figure S6A). RNF5 KD enhanced growth of MDA-MB-231 tumors in BALB/c nude mice relative to control shRNA-expressing tumors (Figure 6E, top). Furthermore, shRNF5 expressing tumors no longer responded to paclitaxel and exhibited elevated SLC1A5/38A2 expression relative to shControl-expressing tumors (Figure 6E, bottom). To directly confirm SLC1A5/38A2 function in tumor growth and response to chemotherapy, we generated MDA-MB-231 cells that stably express shControl, shSLC1A5+shSLC38A2, or shRNF5+shSLC1A5+shSLC38A2. Notably, SLC1A5/38A2 KD attenuated MDA-MB-231 tumor growth (Figures 6F and S6D) and sensitized tumors to paclitaxel treatment. Interestingly, tumors in which SLC1A5/38A2 expression and that of RNF5 were attenuated were slightly smaller than SLC1A5/38A2 KD tumors (Figure 6F), substantiating the important role of RNF5 in the control of these Gln carrier proteins, while pointing to additional possible effects elicited upon RNF5 KD in tumors where SLC1A5/38A2 were already depleted.

Low SLC1A5/38A2 Expression in Tumors Is Associated with Improved Prognosis in Luminal Type Human BCa

We next assessed the significance of the RNF5-SLC1A5/38A2 regulatory axis using a tissue microarray (TMA) consisting of ~538 human BCa cores, all of which had undergone pathological assessment and included annotated clinical outcome. Of those, >350 cores enabled high-quality staining with at least one of the three antibodies (SLC1A5, SLC38A2, and RNF5) that were used in this analysis (Figure 7A). Among characteristic BCa markers, a node-negative state was associated with disease-free survival over 15 years (263 of 538; p value = 7×10^{-12}; Figure S7A). Likewise, estrogen receptor (ER) positivity (both determined based on 2010 American Society of Clinical Oncology/College of American Pathologists criteria) was also associated with good survival over 15 years (252 of 535; p value = 4.3×10^{-5}; Figure S7B). Strikingly, low SLC1A5 expression was significantly associated with an increase in disease-free survival (191 of 366 tumors; p value = 7.5×10^{-5}; Figure 7B). Furthermore, low SLC1A5 and ER^{pos} (119 of 363) or nodes^{neg} (98 of 366) correlated with good prognosis (Figures S7C and S7D). Furthermore, SLC1A5^{lo}/SLC38A2^{lo} (59 of 255 tumors) was significantly associated with increased disease-free survival (p value = 0.0068; Figure S7E). Compared with SLC38A2, low SLC1A5 expression was more strongly associated with positive prognosis (124 of 255 cores; p value = 0.0068; Figure S7E). Lastly, ~23% (79 of 340 tumors) of BCa tumors exhibited RNF5^{hi} and SLC1A5^{lo} expression and were associated with better prognosis than tumors expressing high SLC1A5^{hi} and low RNF5^{lo} (p value = 0.00058; Figure 7C). Notably, SLC1A5^{lo} was associated with positive prognosis, even in the presence of RNF5^{lo}, suggesting that other mechanisms may contribute to SLC1A5^{lo} expression (99 of 340 cases; Figure 7C). The latter may represent RNF5-independent mechanisms, as reflected in lower transcription of the Gln carrier protein (Figure S7F). Significantly, 33.5% (108 of 311 tumors) BCa tumors exhibited RNF5^{hi} and SLC1A5/SLC38A2^{lo}, a pattern strongly associated with increased disease-free survival (p value = 0.0021; Figure 7D). Consistent with these observations, analysis of the reverse-phase protein array (RPPA) data obtained for SLC1A5 on 747 TCGA samples showed that SLC1A5 is

(E) Indicated cell lines were incubated with paclitaxel for indicated times. Cell lysates were immunoblotted with indicated antibodies.
(F) 231 cells were pretreated without or with 1 μM GSK2606414 (a PERK inhibitor) for 2 hr and then incubated with 100 nM paclitaxel for indicated times. WB performed with indicated antibodies.
(G) 231 cells were transfected with SLC1A5-V5, treated with DMSO or 100 nM paclitaxel for 24 hr, and then subjected to labeling with [^{35}S]Met/Cys. SLC1A5-V5 was immunopurified and incubated with BNPS-Skatole in vitro for the indicated time points. [^{35}S]SLC1A5 was detected using autoradiography and quantified with the aid of ImageJ (NIH) software.
(H) 231 cells were transfected with shControl or two different shRNF5s (#1, #2) followed by incubation with 100 nM paclitaxel for 24 hr. WB performed with indicated antibodies.
(I) 231 cells transfected with shControl or shRNF5 were incubated with paclitaxel for 24 hr and then treated with CHX (50 μg/ml) for indicated times. WB performed with indicated antibodies.
(J) 231 cells were transfected with indicated constructs and treated with paclitaxel for 6 hr. Relative ROS levels were determined by DCFDA (2′7′-dichlorodihydrofluorescein diacetate) staining. Bars represent means ± SD of three independent experiments.
See also Figure S4.

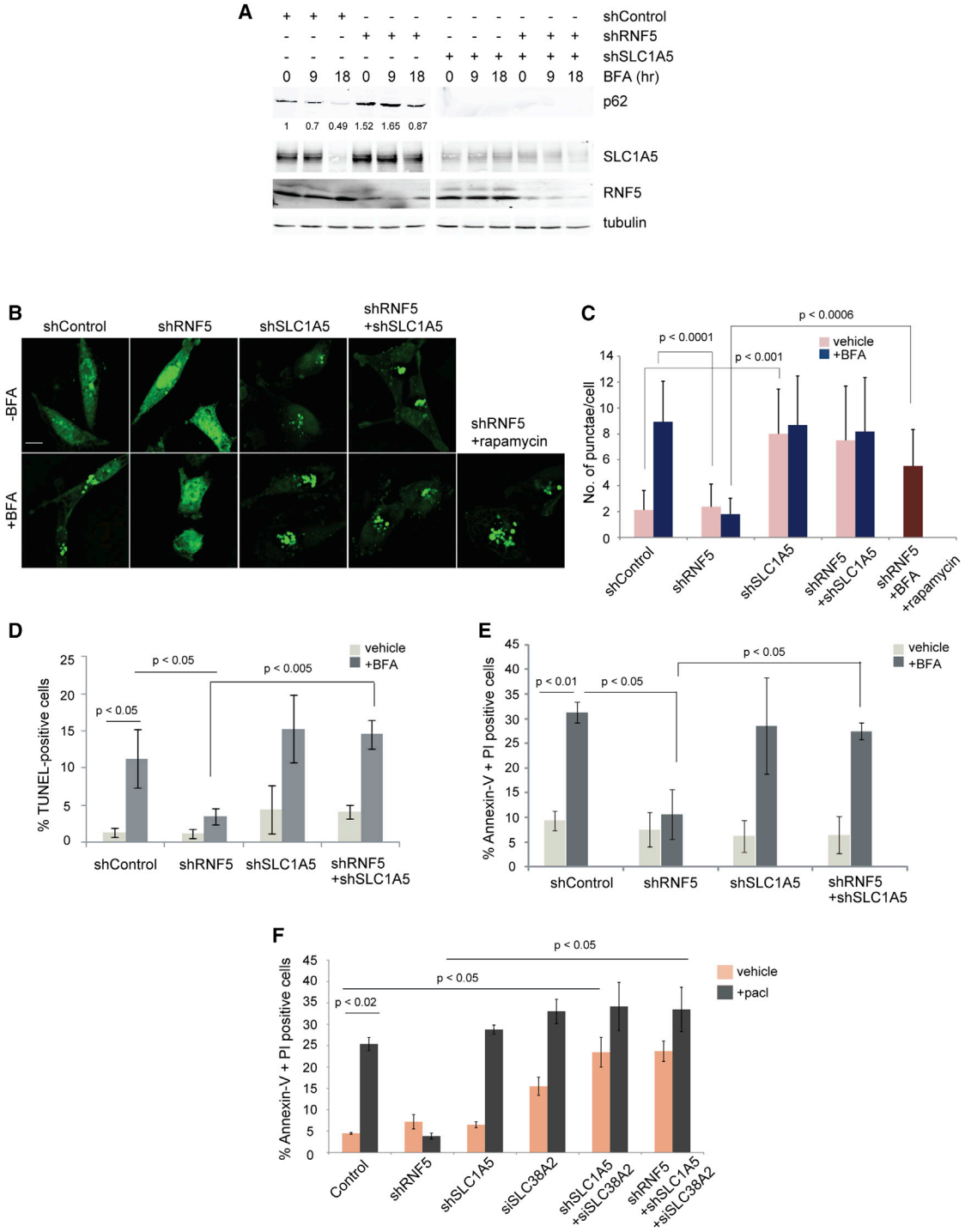

Figure 5. RNF5 Regulation of SLC1A5 Promotes Autophagy and Apoptosis in Response to ERS

(A) MDA-MB-231 cells transfected with indicated constructs were incubated with 2.5 μg/ml BFA for indicated times. WB performed with indicated antibodies.

(B) MDA-MB-231 cells stably expressing the indicated constructs were transfected with a GFP-LC3 expression plasmid and incubated with or without 2.5 μg/ml BFA or with 1 μM rapamycin. Scale bar, 10 μm.

(C) Quantification of GFP-LC3 punctae in cells treated as in (B). Bars represent means of ± SD of triplicate samples of >50 cells analyzed per sample in three experiments. A two-tailed, unpaired t test was used to calculate significance.

(D) MDA-MB-231 cells transfected with indicated constructs were incubated with 2.5 μg/ml BFA for 18 hr, and apoptotic cells were counted using a TUNEL assay. Bars indicate mean values ± SD of three experiments.

(legend continued on next page)

present at high levels (defined by mean and 2 SD) in approximately half of basal-like BCa cells as well as a subset of luminal B BCa cells and at low levels in the newly described reactive BCa subset (Akbani et al., 2014). Based on an analysis of 205 antibodies, SLC1A5 is co-expressed with proteins involved in cellular differentiation and polarity, cellular metabolism, and proliferation and negatively correlated with phosphatidylinositol 3-kinase (PI3K) and mitogen-activated protein kinase (MAPK) pathway signaling (Figure 7E). We also assessed the relationship between SLC1A5 expression and responsiveness to neoadjuvant therapies. Two cohorts of 30 tumors each were obtained from patients receiving a combination of either taxanes with cisplatin or anthracycline with cyclophosphamide as part of neoadjuvant therapy. In both groups, relatively high SLC1A5 expression was associated with poor responsiveness to therapy (data not shown). These observations are consistent with the poor prognosis associated with high SLC1A5 expression seen in the TMA and RPPA sets and confirm data obtained in BCa cultures.

DISCUSSION

Altered metabolism is a hallmark of the genetically and epigenetically driven global rewiring of signaling pathways in cancer cells. Thus, a better understanding of molecular mechanisms underlying these changes should improve our ability to define their contribution to tumor development, progression, and response to therapy. Given the intimate link between metabolic cues and key cellular processes, including ERS, UPR, autophagy, and cell death programs, identifying mechanisms that characterize specific tumor groups may allow design of personalized therapies.

In this study, we identify a role for the ubiquitin E3 ligase RNF5 in regulating L-Gln uptake and mTOR signaling in BCa cells, thereby advancing our understanding of mechanisms underlying metabolic and cellular responses to chemotherapy. ERS-induced protein misfolding likely underlies degradation of SLC1A5 and SLC38A2 by the ER-bound E3 ligase RNF5, resulting in a reduced L-Gln uptake and mTOR signaling, slower growth, and sensitization of BCa cells to autophagy and cell death programs. Inhibition of RNF5 in either *MMTV-PyMT* mouse mammary tumor model or MDA-MB-231 BCa cells promoted tumor growth and, in the case of MDA-MB-231, resistance to paclitaxel treatment. BCa TMA data revealed that higher SLC1A5 and lower RNF5 expression coincides with poorer prognosis and identified a subset of tumors in which high level of RNF5 coincided with poor outcome, consistent with our previous study (Bromberg et al., 2007). Independent studies showed that increased SLC38A2 expression upon amino acid starvation is associated with eIF2α phosphorylation (Gaccioli et al., 2006), suggesting a possible feedback mechanism controlling SLC38A2 levels. Notably, increased SLC38A2 expression seen following hypertonic stress did not require eIF2α phosphorylation, suggesting that diverse mechanisms control SLC38A2 expression. Furthermore, while our studies document effects of ERS-inducing compounds, including TG, on Gln carrier protein degradation, TG reportedly induces expression of SLC1A5/38A2 in pancreatic β-cells (Krokowski et al., 2013), suggesting that regulation of Gln carrier protein is cell-type dependent. Consistent with complex regulation of Gln carrier proteins is the observation that ATF4, a key UPR-transducing protein, binds to the SLC38A2 promoter in HepG2 human hepatoma cells, albeit without altering transcription (Gjymishka et al., 2008). The diverse regulation of Gln carrier proteins is consistent with our observations in cultured BCa cells, TMAs, and RPPAs, where we identified cohorts potentially regulated by distinct mechanisms and that show different clinical outcomes. Importantly, the regulatory axis identified here likely represents about a third of BCa luminal type tumors, supporting consideration of patient stratification for specific therapies.

Growing evidence supports a role for ERS and UPR in tumor biology. Proteins associated with UPR are upregulated in ischemic regions of tumors (Shuda et al., 2003), suggesting that UPR serves a protective function once tumors outstrip their vascular supply. UPR also reportedly plays an important role in *Tsc2*$^{-/-}$ tumors, which show constitutive mTORC1 activity (Young et al., 2013). In that case, increased UPR seen in hypoxic *Tsc2*$^{-/-}$ cells deprived of serum lipids was implicated in IRE1-dependent cell death, which was rescued by addition of unsaturated lipids, arguing for the importance of balanced lipid and protein synthesis in modulating UPR-dependent cell death programs. The latter is consistent with our recent finding that fine-tuning of UPR determines commitment to cell death programs, a process regulated by the ubiquitin ligase Siah1/2 (Scortegagna et al., 2014). ERS-induced UPR also appears integral to the mechanism identified here in which paclitaxel-dependent misfolding underlies RNF5 association with and degradation of Gln carrier proteins. One would predict that RNF5 plays an equally important role in other tumors in which ERS is triggered by chemotherapeutic drugs (Carew et al., 2006; Gills et al., 2007; Phillips et al., 1998).

Our study illustrates that the RNF5-SLC1A5/38A2 pathway is induced by the ability of paclitaxel, but not doxorubicin, to induce ERS. Thus, the dependence on Gln uptake may allow one to distinguish and possibly stratify tumors showing a favorable response to ERS-based therapy based on the status of these regulatory components. RPPA analysis confirmed that high expression of SLC1A5 is associated with basal-like and luminal B types of BCa, as well poorer responsiveness to therapy, whereas low SLC1A5 expression coincided with reactive, luminal type tumors. Along these lines, tumors more dependent on Gln, such as triple-negative BCa cells (Timmerman et al., 2013) and melanoma cells (Filipp et al., 2012), could benefit from therapies that target Gln-pathway components in combination with other therapies. Our data also show that RNF5-mediated control of Gln carrier proteins does not function in all BCa

(E) MDA-MB-231 cells transfected with indicated constructs were incubated with 2.5 μg/ml BFA for 24 hr, stained with Annexin-V-EGFP and PI, and analyzed by FACS. Bars indicate mean values ± SD of three experiments.
(F) MDA-MB-231 cells transfected with indicated constructs were incubated with 100 nM paclitaxel for 48 hr, stained with Annexin-V-EGFP and PI, and analyzed by FACS. Bars indicate mean values ± SD of three experiments.
See also Figure S5.

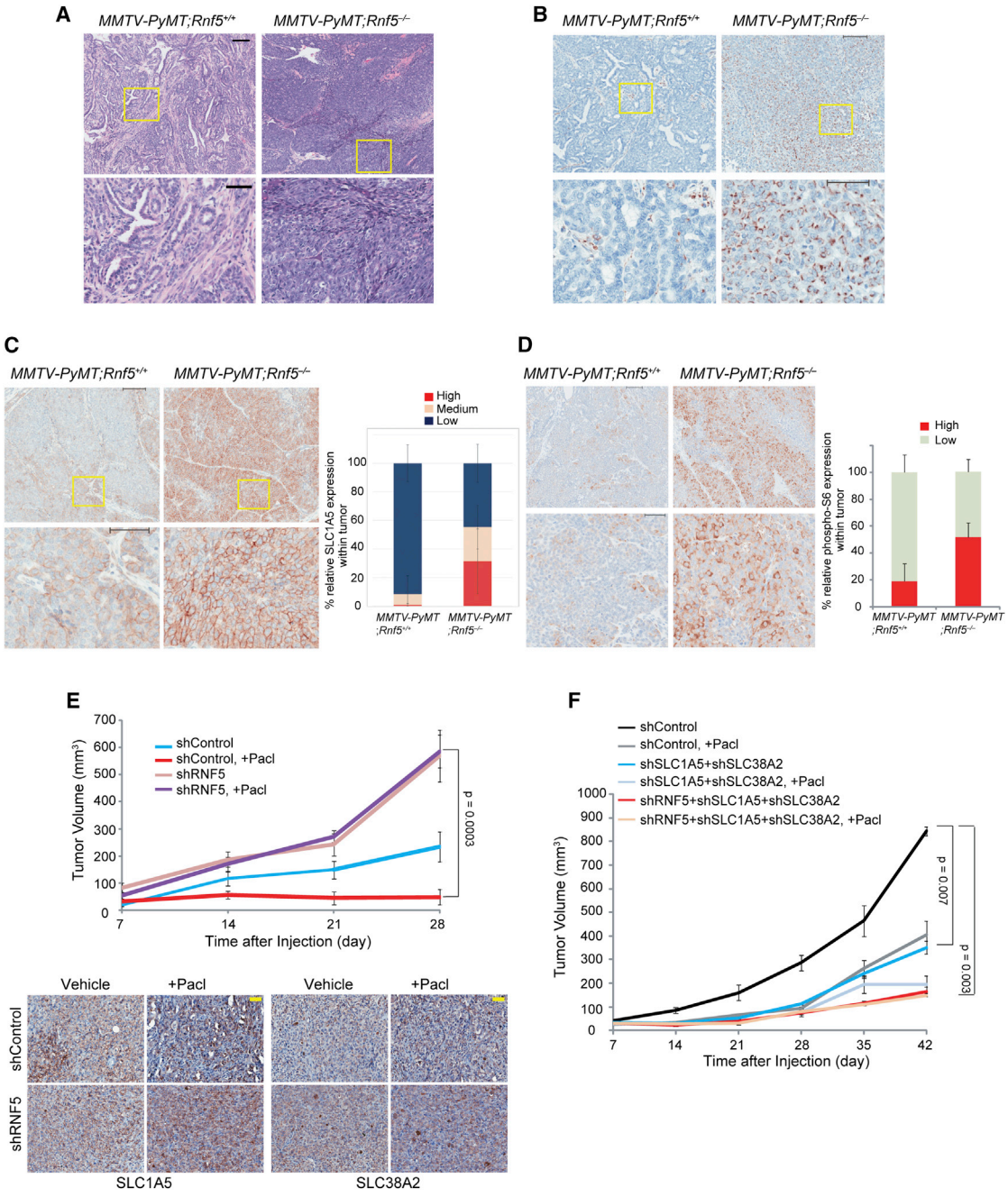

Figure 6. RNF5 Loss Gives Rise to Less Differentiated *MMTV-PyMT* Mammary Tumors, Enhances Human MDA-MB231 BCa Growth, and Reduces Tumor Responses to Paclitaxel

(A and B) H&E staining (A) or immunohistochemistry (IHC) staining of vimentin (B) of mammary tumors from *MMTV-PyMT;Rnf5*$^{+/+}$ or *MMTV-PyMT;Rnf5*$^{-/-}$ mice. Lower panels show higher-magnification images of insets in upper panels. Scale bars, 100 μm (upper panels); 50 μm (lower panels).

(C) Left: IHC staining of SLC1A5 in mammary tumors from indicated genotypes. Scale bars, 100 μm (upper panels); 50 μm (lower panels). Right: quantification of SLC1A5 staining. Bars represent mean values ± SD of groups consisting ten mice each.

(D) Left: IHC staining of phospho-S6 ribosomal protein in mammary tumors from indicated genotypes. Scale bars, 100 μm (upper panels); 50 μm (lower panels). Right: quantification of phospho-S6 ribosomal protein staining. Bars represent mean values ± SD of groups of ten mice.

(E) Top: MDA-MB-231 BCa cells (5 × 10^6) stably expressing shRNF5 or shControl were injected into nude mice, and mice were monitored weekly for tumor growth. Animals were subjected to paclitaxel treatment 7 days after injection, as described in Experimental Procedures. Bars represent ± SEM. Bottom: IHC staining of SLC1A5 or SLC38A2 in tumors generated as indicated in (E). Scale bars, 50 μm.

(F) MDA-MB-231 BCa cells (5 × 10^6) stably expressing indicated constructs were injected as indicated, monitored, and treated as in (E). Bars represent ± SEM. See also Figure S6.

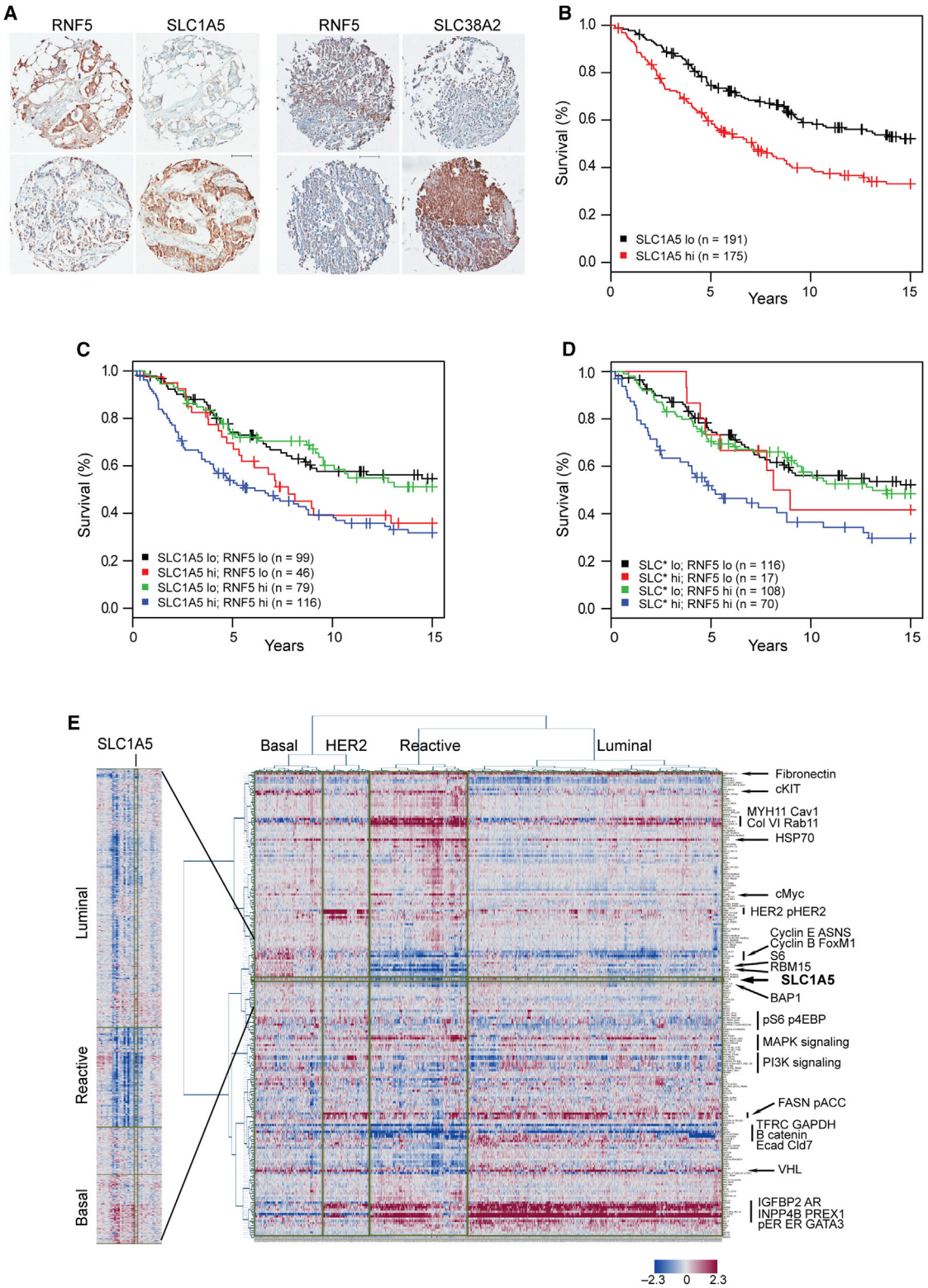

Figure 7. RNF5 and SLC1A5/38A2 Could Serve as Prognostic Markers in Human BCa

(A) Representative immunostaining of a BCa TMA, depicting high and low levels of RNF5, SLC1A5, and SLC38A2 expression. Scale bar, 100 μm.

(B) Kaplan-Meier curves comparing disease-free survival of BCa patients with tumors expressing high or low levels of SLC1A5 protein ($p = 7.5 \times 10^{-5}$).

(C) Kaplan-Meier curves comparing survival of BCa patients with tumors expressing high or low RNF5 together with high or low levels of SLC1A5 ($p = 0.00058$).

(legend continued on next page)

cells and is associated with positive prognosis in a third of all BCa specimens evaluated (and half of BCa samples that express low levels of SLC1A5; reduced transcription of SLC1A5 may underlie regulation in the remaining BCa fraction).

Initial data from cohorts of BCa tumors subjected to neoadjuvant therapy demonstrate that high levels of SLC1A5 coincided with poor prognosis. These findings are consistent with our cell culture and xenograft studies. Noteworthy is that two-thirds of BCa did not maintain RNF5-control of SLC1A5/38A2, attesting to its importance as well as for the diverse mechanisms used by BCa to escape this control process. Mechanisms used to escape RNF5-mediated control of Gln carrier protein expression might include RNF5 inactivation or upregulated transcription of genes encoding SLC1A5/38A2, topics that require further study. Of note, SLC38A2 is reportedly regulated by the ubiquitin ligase Nedd4-2, suggesting interplay between RNF5 and Nedd4-2 ligases (Hatanaka et al., 2006). Certain tumors may fail to activate the RNF5-SLC1A5 pathway because they possess defense mechanisms that more effectively block ERS induction or engage other pathways (such as androgen signaling); those tumors may benefit from chemotherapies that are not dependent on ERS induction. Although our study focused on BCa, the RNF5-SLC1A5/38A2 axis may play an equally important role in other tumor types, particularly those exhibiting L-Gln addiction phenotypes.

Overall, regulation of SLC1A5/38A2 by RNF5 represents a temporally and spatially restricted mechanism to control Gln uptake, as it occurs following ERS (induced by specific chemotherapeutic drugs) and is restricted to membrane domains, where RNF5 is anchored. Our findings substantiate the importance of altered L-Gln uptake in BCa and reveal a mechanism underlying regulation of the L-Gln carrier proteins SLC1A5 and SLC38A2 by the ubiquitin ligase RNF5. Given the clinical implications of low SLC1A5 and SLC38A2 expression for BCa prognosis and the role of RNF5 in regulating stability of these proteins, our findings not only identify a marker potentially useful for BCa patient stratification but also provide a mechanistic basis for differences in Gln metabolism, a key driver of tumor development and response to therapy.

EXPERIMENTAL PROCEDURES

Animal Studies

All animal experiments were approved by Sanford-Burnham's Institutional Animal Care and Use Committee. Animal care was followed according to institutional guidelines. Detailed experimental procedures are provided in the Supplemental Experimental Procedures.

Human Tumor Array Analysis and RPPA

The Yale cohort (n = 649, patients diagnosed 1962–1982) was constructed into a TMA at Yale and represents patients diagnosed at Yale New Haven Hospital. The follow-up information on cases was obtained from the Yale New Haven Tumor Registry, the Yale-New Haven Hospital medical records, and the Connecticut Death Records. Tissues were collected in accordance with consent guidelines using protocol 9503008219 issued to David L. Rimm from the Yale institutional review board (IRB) with patient consent acceptable for the time period of specimen acquisition or waiver of consent. All samples used in the RPPA analysis were obtained by The Cancer Genome Atlas (TCGA) under IRB approvals to obtain tissues and share with the TCGA. The RPPA analysis of the TCGA samples was performed under an MD Anderson Cancer Center IRB approval.

Plasmids and shRNA

Plasmids expressing FLAG-RNF5, FLAG-RNF5 RM, and FLAG-RNF5 ΔCT have been described previously (Bromberg et al., 2007; Tcherpakov et al., 2009). Plasmids expressing SLC1A5-V5 and SLC38A2-V5 were purchased from Arizona State University Biodesign Institute. shRNAs were purchased from Open Biosystems or OriGene. Sequences were as follows: for shRNF5, #1, agc ttt aca tac tgg aca ctc and #2, gac, aac, ctt, ctc, tct, gct, gat; for shSLC1A5, ttc act tgt atc aac tca ggc; and for shSLC38A2, aat cca aat gcc tta tat c. The RNAi Consortium lentiviral pLKO.1 control vector served as the shControl. The human SLC38A2 siGENOME SMARTpool (D-007559-01, D-007559-02, D-007559-03, D-007559-04) and SiGENOME nontargeting small interfering RNA (siRNA; D-001206-13-05) were purchased from Open Biosystems.

Cell Lines and Transfections

MCF7 cells were cultured in DMEM containing 10% fetal bovine serum (FBS). MDA-MB-231, MDA-MB-453, SKBR-3, T47D, and MDA-MB-468 cells were maintained in RPMI medium containing 10% FBS. Cells were transfected with plasmids and shRNAs using JetPrime (PolyPlus) and with siRNAs using the DharmaFECT1 transfection reagent (Open Biosystems).

Antibodies and Chemicals

The anti-RNF5 antibody was described previously (Bromberg et al., 2007; Delaunay et al., 2008). Other antibodies were obtained from the following sources: SLC1A5 (Santa Cruz Biotechnology sc-99002 and Sigma HPA035240); vimentin (Sigma HPA001762); SLC38A2 (Santa Cruz sc-67081 and Sigma HPA035180); phospho-mTOR (2971), phospho-S6K1 (9206), phospho-S6 (4857), phospho-4EBP1 (9459), mTOR (2972), S6K1 (9202), 4EBP1 (9644), phospho-eIF2α (9721), eIF2α (9722), IREα (3294), PDI (3501), Ero1-Lα (3264), calnexin (2433) (all from Cell Signaling Technology); BiP (Santa Cruz sc-13968); phospho-IREα (Novus Biologicals NB100-2323); p62 (BD Biosciences 610832); V5 (Invitrogen 46-0705); and FLAG (Sigma F1804). BFA was purchased from eBiosciences. TM, TG, cisplatin, doxorubicin, and paclitaxel were purchased from Sigma.

Immunoprecipitation

Cells were lysed in 50 mM Tris-HCl (pH 8) containing 150 mM NaCl, 1 mM PMSF, 1× protease inhibitor cocktail (Roche), and 1% Triton X-100 or 0.5% Nonidet P-40. Cell lysates were incubated with appropriate antibodies for 3 hr at 4°C, and then 20 μl of protein A/G agarose beads (Santa Cruz) was added, and lysates were incubated for an additional 2 hr. Western blots (WBs) were analyzed and quantified with the aid of the Odyssey imaging scanner (LI-COR Biosciences).

Cell Growth and Clonogenic Assay

For the cell growth assay, cells (2.5×10^5) were seeded in triplicate in 60-mm plates for 24 hr. Cells were then treated with BFA (2.5 μg/ml) for 18 hr before harvesting. Viable cells were counted following trypan blue staining. For the clonogenic assay, cells were plated in six-well plates at 400 cells/2 ml of medium per well. The medium was not changed during the experiment. After 7–10 days, colonies were fixed, stained with crystal violet, and counted.

SUPPLEMENTAL INFORMATION

Supplemental Information includes Supplemental Experimental Procedures and seven figures and can be found with this article online at http://dx.doi.org/10.1016/j.ccell.2015.02.006.

(D) Kaplan-Meier curves comparing survival of BCa patients with tumors expressing high or low RNF5 together with high or low levels of both SLC1A5 and SLC38A2 (SLC* indicates conditions in which both SLC1A5 and SLC38A2 protein levels were either high or low) (p = 0.0021).
(E) Heatmap depicting expression of SLC1A5 among basal-like, HER2-positive, reactive, and luminal BCa in a cohort of 747 samples.
See also Figure S7.

AUTHOR CONTRIBUTIONS

Y.J.J. designed and performed experiments and analyzed data. S.K. analyzed TMA data. B.R. and D.A.S. performed metabolic experiments and analyzed data. A.L.O. and J.W.S. designed, analyzed, and wrote metabolic studies. Y.K., F.P., and T.J. performed bioinformatics analyses of the TMA data. Y.F. and C.R. performed mouse models studies. E.L. and H.K. performed cell-cycle studies and analyzed data. L.M.B. performed MS analyses. R.D.C. performed analyses of tumor histology and pathology. G.B.M. assisted with bioinformatics and data analysis. D.L.R. generated and provided the TMA. Z.A.R. designed experiments, analyzed data, wrote the manuscript, and oversaw generation of reagents and work with collaborators.

ACKNOWLEDGMENTS

We thank Dr. Chin Ha Chung (School of Biological Sciences, Seoul National University, Seoul Korea) for kindly providing BCa cell lines, Dr. Robert Oshima for valuable comments, and members of the Z.A.R. lab for helpful discussions. This work was supported by NIH grants CA097105 and CA128814 to Z.A.R. Support from the Flow Cytometry (Dr. Yoav Altman) and Functional Genomics (Dr. Pedro Aza-Blanc) cores and the Cancer Center Support Grant (P30 CA30199) is acknowledged.

Received: April 29, 2014
Revised: October 28, 2014
Accepted: February 5, 2015
Published: March 9, 2015

REFERENCES

Akbani, R., Ng, P.K., Werner, H.M., Shahmoradgoli, M., Zhang, F., Ju, Z., Liu, W., Yang, J.Y., Yoshihara, K., Li, J., et al. (2014). A pan-cancer proteomic perspective on The Cancer Genome Atlas. Nat. Commun. *5*, 3887.

B'chir, W., Maurin, A.C., Carraro, V., Averous, J., Jousse, C., Muranishi, Y., Parry, L., Stepien, G., Fafournoux, P., and Bruhat, A. (2013). The eIF2α/ATF4 pathway is essential for stress-induced autophagy gene expression. Nucleic Acids Res. *41*, 7683–7699.

Baird, F.E., Bett, K.J., MacLean, C., Tee, A.R., Hundal, H.S., and Taylor, P.M. (2009). Tertiary active transport of amino acids reconstituted by coexpression of System A and L transporters in Xenopus oocytes. Am. J. Physiol. Endocrinol. Metab. *297*, E822–E829.

Bernasconi, R., Galli, C., Kokame, K., and Molinari, M. (2013). Autoadaptive ER-associated degradation defines a preemptive unfolded protein response pathway. Mol. Cell *52*, 783–793.

Blommaart, E.F., Luiken, J.J., Blommaart, P.J., van Woerkom, G.M., and Meijer, A.J. (1995). Phosphorylation of ribosomal protein S6 is inhibitory for autophagy in isolated rat hepatocytes. J. Biol. Chem. *270*, 2320–2326.

Bromberg, K.D., Kluger, H.M., Delaunay, A., Abbas, S., DiVito, K.A., Krajewski, S., and Ronai, Z. (2007). Increased expression of the E3 ubiquitin ligase RNF5 is associated with decreased survival in breast cancer. Cancer Res. *67*, 8172–8179.

Carew, J.S., Nawrocki, S.T., Krupnik, Y.V., Dunner, K., Jr., McConkey, D.J., Keating, M.J., and Huang, P. (2006). Targeting endoplasmic reticulum protein transport: a novel strategy to kill malignant B cells and overcome fludarabine resistance in CLL. Blood *107*, 222–231.

DeBerardinis, R.J., Mancuso, A., Daikhin, E., Nissim, I., Yudkoff, M., Wehrli, S., and Thompson, C.B. (2007). Beyond aerobic glycolysis: transformed cells can engage in glutamine metabolism that exceeds the requirement for protein and nucleotide synthesis. Proc. Natl. Acad. Sci. USA *104*, 19345–19350.

Delaunay, A., Bromberg, K.D., Hayashi, Y., Mirabella, M., Burch, D., Kirkwood, B., Serra, C., Malicdan, M.C., Mizisin, A.P., Morosetti, R., et al. (2008). The ER-bound RING finger protein 5 (RNF5/RMA1) causes degenerative myopathy in transgenic mice and is deregulated in inclusion body myositis. PLoS One *3*, e1609.

Evans, K., Nasim, Z., Brown, J., Clapp, E., Amin, A., Yang, B., Herbert, T.P., and Bevington, A. (2008). Inhibition of SNAT2 by metabolic acidosis enhances proteolysis in skeletal muscle. J. Am. Soc. Nephrol. *19*, 2119–2129.

Filipp, F.V., Ratnikov, B., De Ingeniis, J., Smith, J.W., Osterman, A.L., and Scott, D.A. (2012). Glutamine-fueled mitochondrial metabolism is decoupled from glycolysis in melanoma. Pigment Cell Melanoma Res. *25*, 732–739.

Fluck, M.M., and Schaffhausen, B.S. (2009). Lessons in signaling and tumorigenesis from polyomavirus middle T antigen. Microbiol. Mol. Biol. Rev. *73*, 542–563.

Fuchs, B.C., Finger, R.E., Onan, M.C., and Bode, B.P. (2007). ASCT2 silencing regulates mammalian target-of-rapamycin growth and survival signaling in human hepatoma cells. Am. J. Physiol. Cell Physiol. *293*, C55–C63.

Gaccioli, F., Huang, C.C., Wang, C., Bevilacqua, E., Franchi-Gazzola, R., Gazzola, G.C., Bussolati, O., Snider, M.D., and Hatzoglou, M. (2006). Amino acid starvation induces the SNAT2 neutral amino acid transporter by a mechanism that involves eukaryotic initiation factor 2alpha phosphorylation and cap-independent translation. J. Biol. Chem. *281*, 17929–17940.

Gao, P., Tchernyshyov, I., Chang, T.C., Lee, Y.S., Kita, K., Ochi, T., Zeller, K.I., De Marzo, A.M., Van Eyk, J.E., Mendell, J.T., and Dang, C.V. (2009). c-Myc suppression of miR-23a/b enhances mitochondrial glutaminase expression and glutamine metabolism. Nature *458*, 762–765.

Gills, J.J., Lopiccolo, J., Tsurutani, J., Shoemaker, R.H., Best, C.J., Abu-Asab, M.S., Borojerdi, J., Warfel, N.A., Gardner, E.R., Danish, M., et al. (2007). Nelfinavir, A lead HIV protease inhibitor, is a broad-spectrum, anticancer agent that induces endoplasmic reticulum stress, autophagy, and apoptosis in vitro and in vivo. Clin. Cancer Res. *13*, 5183–5194.

Gjymishka, A., Palii, S.S., Shan, J., and Kilberg, M.S. (2008). Despite increased ATF4 binding at the C/EBP-ATF composite site following activation of the unfolded protein response, system A transporter 2 (SNAT2) transcription activity is repressed in HepG2 cells. J. Biol. Chem. *283*, 27736–27747.

Grove, D.E., Fan, C.Y., Ren, H.Y., and Cyr, D.M. (2011). The endoplasmic reticulum-associated Hsp40 DNAJB12 and Hsc70 cooperate to facilitate RMA1 E3-dependent degradation of nascent CFTRDeltaF508. Mol. Biol. Cell *22*, 301–314.

Hassanein, M., Hoeksema, M.D., Shiota, M., Qian, J., Harris, B.K., Chen, H., Clark, J.E., Alborn, W.E., Eisenberg, R., and Massion, P.P. (2013). SLC1A5 mediates glutamine transport required for lung cancer cell growth and survival. Clin. Cancer Res. *19*, 560–570.

Hatanaka, T., Hatanaka, Y., and Setou, M. (2006). Regulation of amino acid transporter ATA2 by ubiquitin ligase Nedd4-2. J. Biol. Chem. *281*, 35922–35930.

He, C., and Klionsky, D.J. (2009). Regulation mechanisms and signaling pathways of autophagy. Annu. Rev. Genet. *43*, 67–93.

Hetz, C., Chevet, E., and Harding, H.P. (2013). Targeting the unfolded protein response in disease. Nat. Rev. Drug Discov. *12*, 703–719.

Hotamisligil, G.S. (2010). Endoplasmic reticulum stress and the inflammatory basis of metabolic disease. Cell *140*, 900–917.

Kim, S.G., Buel, G.R., and Blenis, J. (2013). Nutrient regulation of the mTOR complex 1 signaling pathway. Mol. Cells *35*, 463–473.

Krokowski, D., Han, J., Saikia, M., Majumder, M., Yuan, C.L., Guan, B.J., Bevilacqua, E., Bussolati, O., Bröer, S., Arvan, P., et al. (2013). A self-defeating anabolic program leads to β-cell apoptosis in endoplasmic reticulum stress-induced diabetes via regulation of amino acid flux. J. Biol. Chem. *288*, 17202–17213.

Kuang, E., Okumura, C.Y., Sheffy-Levin, S., Varsano, T., Shu, V.C., Qi, J., Niesman, I.R., Yang, H.J., López-Otín, C., Yang, W.Y., et al. (2012). Regulation of ATG4B stability by RNF5 limits basal levels of autophagy and influences susceptibility to bacterial infection. PLoS Genet. *8*, e1003007.

Liu, W., Le, A., Hancock, C., Lane, A.N., Dang, C.V., Fan, T.W., and Phang, J.M. (2012). Reprogramming of proline and glutamine metabolism contributes to the proliferative and metabolic responses regulated by oncogenic transcription factor c-MYC. Proc. Natl. Acad. Sci. USA *109*, 8983–8988.

Mariño, G., Niso-Santano, M., Baehrecke, E.H., and Kroemer, G. (2014). Self-consumption: the interplay of autophagy and apoptosis. Nat. Rev. Mol. Cell Biol. *15*, 81–94.

Medina, M.A. (2001). Glutamine and cancer. J Nutr *131*, 2539S–2542S, discussion 2550S–2531S.

Meusser, B., Hirsch, C., Jarosch, E., and Sommer, T. (2005). ERAD: the long road to destruction. Nat. Cell Biol. *7*, 766–772.

Nicklin, P., Bergman, P., Zhang, B., Triantafellow, E., Wang, H., Nyfeler, B., Yang, H., Hild, M., Kung, C., Wilson, C., et al. (2009). Bidirectional transport of amino acids regulates mTOR and autophagy. Cell *136*, 521–534.

Ogata, M., Hino, S., Saito, A., Morikawa, K., Kondo, S., Kanemoto, S., Murakami, T., Taniguchi, M., Tanii, I., Yoshinaga, K., et al. (2006). Autophagy is activated for cell survival after endoplasmic reticulum stress. Mol. Cell. Biol. *26*, 9220–9231.

Okudaira, H., Shikano, N., Nishii, R., Miyagi, T., Yoshimoto, M., Kobayashi, M., Ohe, K., Nakanishi, T., Tamai, I., Namiki, M., and Kawai, K. (2011). Putative transport mechanism and intracellular fate of trans-1-amino-3-18F-fluorocyclobutanecarboxylic acid in human prostate cancer. J. Nucl. Med. *52*, 822–829.

Phillips, L.R., Wolfe, T.L., Malspeis, L., and Supko, J.G. (1998). Analysis of brefeldin A and the prodrug breflate in plasma by gas chromatography with mass selective detection. J. Pharm. Biomed. Anal. *16*, 1301–1309.

Ron, D., and Walter, P. (2007). Signal integration in the endoplasmic reticulum unfolded protein response. Nat. Rev. Mol. Cell Biol. *8*, 519–529.

Scortegagna, M., Kim, H., Li, J.L., Yao, H., Brill, L.M., Han, J., Lau, E., Bowtell, D., Haddad, G., Kaufman, R.J., and Ronai, Z.A. (2014). Fine tuning of the UPR by the ubiquitin ligases Siah1/2. PLoS Genet. *10*, e1004348.

Shore, G.C., Papa, F.R., and Oakes, S.A. (2011). Signaling cell death from the endoplasmic reticulum stress response. Curr. Opin. Cell Biol. *23*, 143–149.

Shuda, M., Kondoh, N., Imazeki, N., Tanaka, K., Okada, T., Mori, K., Hada, A., Arai, M., Wakatsuki, T., Matsubara, O., et al. (2003). Activation of the ATF6, XBP1 and grp78 genes in human hepatocellular carcinoma: a possible involvement of the ER stress pathway in hepatocarcinogenesis. J. Hepatol. *38*, 605–614.

Tabas, I., and Ron, D. (2011). Integrating the mechanisms of apoptosis induced by endoplasmic reticulum stress. Nat. Cell Biol. *13*, 184–190.

Taylor, R.W., Jobling, M.S., Turnbull, D.M., and Chinnery, P.F. (2003). Frequency of rare mitochondrial DNA mutations in patients with suspected Leber's hereditary optic neuropathy. J. Med. Genet. *40*, e85.

Tcherpakov, M., Delaunay, A., Toth, J., Kadoya, T., Petroski, M.D., and Ronai, Z.A. (2009). Regulation of endoplasmic reticulum-associated degradation by RNF5-dependent ubiquitination of JNK-associated membrane protein (JAMP). J. Biol. Chem. *284*, 12099–12109.

Timmerman, L.A., Holton, T., Yuneva, M., Louie, R.J., Padró, M., Daemen, A., Hu, M., Chan, D.A., Ethier, S.P., van 't Veer, L.J., et al. (2013). Glutamine sensitivity analysis identifies the xCT antiporter as a common triple-negative breast tumor therapeutic target. Cancer Cell *24*, 450–465.

Walter, P., and Ron, D. (2011). The unfolded protein response: from stress pathway to homeostatic regulation. Science *334*, 1081–1086.

Wang, J.B., Erickson, J.W., Fuji, R., Ramachandran, S., Gao, P., Dinavahi, R., Wilson, K.F., Ambrosio, A.L., Dias, S.M., Dang, C.V., and Cerione, R.A. (2010). Targeting mitochondrial glutaminase activity inhibits oncogenic transformation. Cancer Cell *18*, 207–219.

Willems, L., Jacque, N., Jacquel, A., Neveux, N., Maciel, T.T., Lambert, M., Schmitt, A., Poulain, L., Green, A.S., Uzunov, M., et al. (2013). Inhibiting glutamine uptake represents an attractive new strategy for treating acute myeloid leukemia. Blood *122*, 3521–3532.

Wise, D.R., DeBerardinis, R.J., Mancuso, A., Sayed, N., Zhang, X.Y., Pfeiffer, H.K., Nissim, I., Daikhin, E., Yudkoff, M., McMahon, S.B., and Thompson, C.B. (2008). Myc regulates a transcriptional program that stimulates mitochondrial glutaminolysis and leads to glutamine addiction. Proc. Natl. Acad. Sci. USA *105*, 18782–18787.

Witte, D., Ali, N., Carlson, N., and Younes, M. (2002). Overexpression of the neutral amino acid transporter ASCT2 in human colorectal adenocarcinoma. Anticancer Res. *22*, 2555–2557.

Young, R.M., Ackerman, D., Quinn, Z.L., Mancuso, A., Gruber, M., Liu, L., Giannoukos, D.N., Bobrovnikova-Marjon, E., Diehl, J.A., Keith, B., and Simon, M.C. (2013). Dysregulated mTORC1 renders cells critically dependent on desaturated lipids for survival under tumor-like stress. Genes Dev. *27*, 1115–1131.

Younger, J.M., Chen, L., Ren, H.Y., Rosser, M.F., Turnbull, E.L., Fan, C.Y., Patterson, C., and Cyr, D.M. (2006). Sequential quality-control checkpoints triage misfolded cystic fibrosis transmembrane conductance regulator. Cell *126*, 571–582.